

## Chemistry Inside Carbon Nanotubes: the Menshutkin S<sub>N</sub>2 Reaction

Mathew D. Halls<sup>†</sup> and H. Bernhard Schlegel\*

Department of Chemistry and Institute for Scientific Computing, Wayne State University,  
Detroit, Michigan 48202

Received: October 4, 2001

In an effort to gain insight into the effect of carbon nanotube confinement on reaction enthalpies and activation energies, calculations using hybrid density functional theory have been carried out for the Menshutkin S<sub>N</sub>2 reaction in gas phase and inside carbon nanotubes. The polarizability of the carbon nanotubes provides an interaction mechanism, which leads to the stabilization of confined dipolar species. Inside hydrogen-terminated (8,0) and (9,0) carbon nanotubes, the activation energy and reaction endothermicity for the Menshutkin S<sub>N</sub>2 reaction are significantly reduced compared to those in the gas phase. Polarizable continuum models, using dielectric constants calculated from the carbon nanotube polarizabilities, are found to provide results in remarkable agreement with all electron nanotube-confined calculations, confirming the stabilization mechanism and offering a cost-effective approach for further exploration of the effects of the carbon nanotube environment. Overall, the effect of carbon nanotube confinement on reaction enthalpies closely resembles solvation in a low-dielectric solvent. Therefore, chemical reactions in which there is a separation of charge along the reaction coordinate may be enhanced inside fullerene-based materials because of their large electronic polarizabilities.

### Introduction

Since their discovery by Iijima in 1991,<sup>1</sup> carbon nanotubes have become the focus of intense scientific investigation<sup>2–5</sup> because of their remarkable mechanical<sup>6–9</sup> and electronic properties.<sup>10–13</sup> In addition to their interesting physical properties, carbon nanotubes are structurally well defined in terms of chirality and tube diameter, making them a unique nanoscale environment in which chemical reactions may be carried out. Compared to the gas phase, reaction energetics, mechanism, and dynamics could be significantly altered inside of carbon nanotubes because of their large electronic polarizabilities and because of the severely reduced reaction volume. The use of carbon nanotubes as nanoscale reaction vessels is an exciting possibility.

Experimentally, carbon nanotubes have been filled with a variety of materials. Ugarte et al.<sup>14</sup> filled carbon nanotubes with molten AgNO<sub>3</sub> and then created pure Ag particles inside the nanotubes by electron-beam-mediated reduction. Carbon nanotubes have also been filled with materials such as KI,<sup>15</sup> Ag, Au, AuCl,<sup>16</sup> ZrCl<sub>4</sub>,<sup>17</sup> and even C<sub>60</sub> and higher fullerenes.<sup>18–23</sup> Inorganic nanorods have been synthesized through carbon nanotube confined reactions. For example, Ga<sub>2</sub>O vapor and NH<sub>3</sub> were reacted inside carbon nanotubes to create GaN nanorods with diameters determined by the radius of the nanotubes.<sup>24</sup> Si<sub>3</sub>N<sub>4</sub> nanorods were also synthesized in a similar fashion.<sup>24</sup>

In the condensed phase, chemical reactivity can change dramatically because of the polarizability of the surrounding medium. In solution, dipolar reactions can be either suppressed or enhanced depending on the nature of charge separation and the reaction symmetry. It is reasonable to expect that confinement inside carbon nanotubes might have similar effects, given their large electronic polarizabilities.

In theoretical investigations examining medium effects on chemical reactivity, the Menshutkin S<sub>N</sub>2 reaction<sup>25,26</sup> is often studied.<sup>27–31</sup> Menshutkin reactions, in which the reactants are neutral and the product species are formally charged, are quite sensitive to the polarity of the surrounding environment, becoming more favorable with increasing polarizability, which stabilizes the separation of charge throughout the reaction. Medium effects, even in a solvent with a very low dielectric constant, result in a reduction in reaction barrier and a decrease in overall endothermicity. Consider, for example, a theoretical study by Rivail and co-workers,<sup>32</sup> in which the reaction barrier and overall endothermicity for H<sub>3</sub>N + H<sub>3</sub>CCl in a solvent with a dielectric constant of only  $\epsilon = 1.88$  (*n*-hexane) were reduced by ca. 9 and 63 kcal/mol from gas phase, respectively.

In the present study, the effect of confinement inside carbon nanotubes on chemical reaction enthalpies and activation energies is investigated. Calculations are carried out for the simplest Menshutkin S<sub>N</sub>2 reaction in the gas phase and inside (8,0) and (9,0) carbon nanotubes for comparison. The proximity effect of the dipolar stabilization of fullerene materials is estimated using a model graphitic sheet. Also, the stabilization mechanism and the effectiveness of a polarizable continuum model to represent the effects of nanotube confinement are examined.

### Theoretical Methods

The calculations described here were performed using the Gaussian suite of programs.<sup>33</sup> The calculations were carried out using the B3PW91 hybrid density functional, corresponding to Becke's three-parameter exchange functional (B3)<sup>34</sup> with Perdew and Wang's gradient-corrected correlation functional (PW91).<sup>35</sup> The molecular reaction system was represented with the 6-31G split valence basis set, augmented with one set of diffuse and one set of polarization functions on heavy atoms, 6-31+G\*,<sup>36–38</sup> and the carbon nanotubes were represented with the 3-21G split valence basis set.<sup>39,40</sup> Transition state optimizations in a polariz-

\* To whom correspondence should be addressed. E-mail: hbs@chem.wayne.edu.

<sup>†</sup> Present Address: Scientific Simulation and Modeling Group, Zyvex Corporation, Richardson, Texas, 75081.

**TABLE 1: Gas-Phase and Polarizable Continuum Model Critical Point Geometric Parameters and Energies for the Menshutkin  $S_N2$  Reaction Computed Using the B3PW91/6-31+G\* Level of Theory**

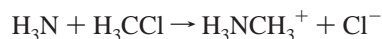
	$R_{C-N}$ (Å)	$R_{C-Cl}$ (Å)	$\angle HCCl$ (deg)	$\mu$ (D)	$E_{SCF}$ (au)	$E_{rel}^a$ (kcal/mol)
Gas Phase						
separated $NH_3$ and $H_3CCl$		1.790	108.7	3.99	-556.578 349	1.2
$H_3N \cdots H_3CCl$	3.512	1.795	108.9	4.38	-556.580 257	0.0
$[H_3N \cdots H_3C \cdots Cl]^+$	1.773	2.515	79.7	13.42	-556.528 187	32.7
$H_3NCH_3^+ \cdots Cl^-$	1.580	2.756	72.7	16.17	-556.529 771	31.7
PCM ( $\epsilon = 2.876$ )						
$[H_3N \cdots H_3C \cdots Cl]^{+b}$	2.006	2.354	87.7	12.57	-556.555 216	17.7 <sup>c</sup>
PCM ( $\epsilon = 2.410$ )						
$[H_3N \cdots H_3C \cdots Cl]^{+b}$	1.979	2.371	86.8	12.68	-556.552 299	19.2 <sup>c</sup>

<sup>a</sup> Relative energies calculated with respect to the reactant dipole complex. <sup>b</sup> Structure optimized using the Onsager model and subsequent energy computed using IPCM. <sup>c</sup> Estimated from IPCM energies for structures early on the reaction path.

able medium were carried out using the Onsager dipole model,<sup>41</sup> and for comparison with the all electron nanotube calculations, single-point calculations were carried out using the isodensity polarizable continuum model (IPCM).<sup>42</sup>

## Results and Discussion

**Gas-Phase Menshutkin  $S_N2$  Reaction.** The Menshutkin  $S_N2$  reaction studied in the present work is the simplest system in which an amine is alkylated by an alkyl halide. Choosing ammonia as the nucleophile and methyl chloride as the methyl transfer reagent gives chloride as the anionic leaving group.



The gas-phase energies and relevant structural parameters computed at the B3PW91/6-31+G\* level of theory are presented in Table 1. Hybrid density functional theory along with the 6-31+G\* basis set has recently been shown to perform very well in describing Menshutkin reactions.<sup>27</sup> The critical points were optimized enforcing  $C_{3v}$  symmetry and were verified by subsequent frequency calculations. The reaction profile for the Menshutkin  $S_N2$  reaction is an asymmetric double-well potential. The first minimum corresponds to a reactant dipole complex formed as the separated reactant molecules approach and their dipole moments align. The reactant dipole complex is only 1.2 kcal/mol lower in energy than the separated reactants, and association has a very small effect on the structural parameters as shown in Table 1. The transition state lies 32.7 kcal/mol higher in energy than the reactant dipole complex. The geometric parameters in Table 1 show a transition state late on the reaction coordinate, as indicated by the advanced degree of hydrogen inversion about the central carbon atom and the extended carbon-chlorine bond. The second minimum corresponds to an ion pair product that is similar in structure to the transition state and only slightly more stable (ca. 1 kcal/mol). The B3PW91/6-31+G\* results described here are in excellent agreement with those reported by Castejon and Wiberg using a comparable level of theory, which was found to agree very well with experimental data.<sup>27</sup>

A reaction path linking the reactant dipole complex and the product ion pair was calculated by performing a series of constrained optimizations, systematically varying the ammonia-methyl N-C bond length ( $R_{N-C}$ ). The gas-phase Menshutkin reaction path is shown in Figure 1. From Table 1 and Figure 1, it can be seen that the gas-phase Menshutkin  $S_N2$  process is quite endothermic, ca. 32 kcal/mol, with a sizable reaction barrier, ca. 33 kcal/mol. The dipole moments of the reactant complex, transition state, and ion pair are calculated to be 4.38, 13.42, and 16.17 D, respectively. A profile of the dipole moment

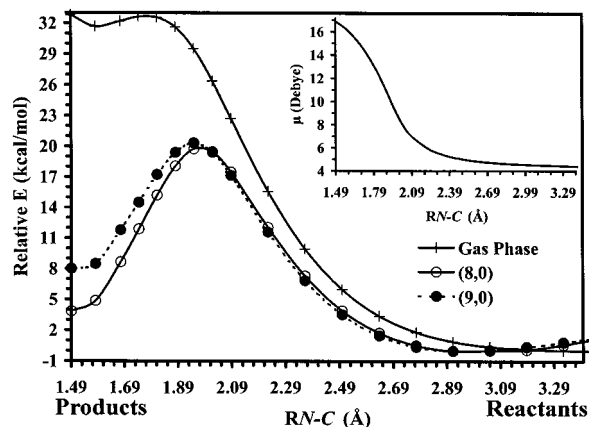


**Figure 1.** Gas-phase potential energy curve for the Menshutkin  $S_N2$  reaction and energy curves for the gas-phase structures inside (8,0) and (9,0) carbon nanotubes, for comparison. The inset shows the profile of the dipole moment along the path linking reactants and products for the Menshutkin reaction.

along the path linking reactants and products is also shown in Figure 1 (inset). As evident from the increasing dipole moment, the separation of charge during the course of this reaction is quite large, providing the opportunity for enormous stabilization in polarizable condensed media.

**Effect of Carbon Nanotube Environment.** A carbon nanotube may be considered as a hollow cylinder formed by rolling up a graphite sheet. The chirality and diameter of a carbon nanotube is uniquely defined by a vector  $(n, m) = na + mb$ ; where  $a$  and  $b$  denote the unit vectors of the hexagonal lattice and  $n$  and  $m$  are integers. The hydrogen-terminated carbon nanotubes used in this work are the (8,0) and (9,0) zigzag nanotubes with stoichiometries of  $C_{96}H_{16}$  and  $C_{108}H_{18}$ , respectively. The carbon nanotubes were fully optimized at the B3PW91/3-21G level of theory, enforcing  $D_{8h}$  and  $D_{9h}$  symmetry. The average diameters of the optimized nanotubes are 6.35 and 7.12 Å for the (8,0) and (9,0) nanotubes, and the C to C length of the nanotubes is 11.37 Å.

The electronic polarizability of carbon nanotubes has been the subject of numerous studies because of their potential use as novel photonic materials and molecular electronic elements.<sup>43-45</sup> The axial polarizability of carbon nanotubes has been found to be much larger than the radial polarizability and is dependent on nanotube length.<sup>43-45</sup> Dipolar species confined within or in the interstitial spaces between carbon nanotubes can interact with an induced image dipole becoming stabilized relative to the gas phase.

To examine this effect, the optimized structures lying on the reaction path linking reactants and products were placed at the center of the optimized nanotubes and single-point energy

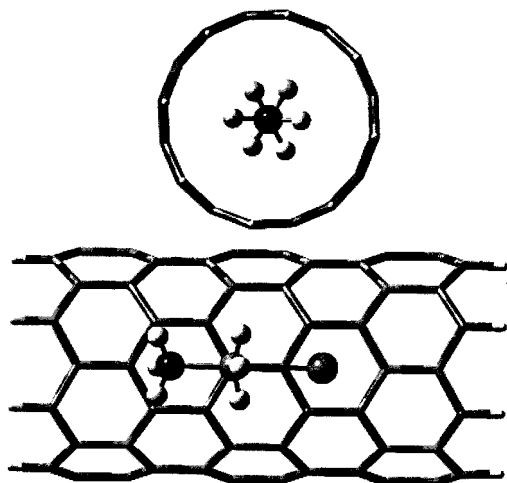


**Figure 2.** Menshutkin  $S_N2$  ion pair product structure inside the (8,0) carbon nanotube as viewed down the symmetry axis of the nanotube (top) and from the side (bottom, nanotube sidewall removed for clarity).

calculations were performed to evaluate changes in the relative energies compared to the gas phase. The Menshutkin system and the carbon nanotubes were represented by the 6-31+G\* and 3-21G basis sets, respectively. The centers of mass and symmetry axes of the reaction structures were aligned with those of the carbon nanotubes, as shown for the ion pair product inside the (8,0) nanotube in Figure 2. The potential energy profiles inside the (8,0) and (9,0) carbon nanotubes are shown in Figure 1 for comparison with the gas-phase results. The gas-phase curve shows a very asymmetric double-well potential with a late transition state having a reaction barrier of ca. 33 kcal/mol, with the overall process being significantly endothermic. Inside the carbon nanotubes, the relative energies change dramatically. First, the ion pair structure is much more stable relative to the reactant dipole complex, making the overall reaction more favorable. Within the (8,0) and (9,0) carbon nanotubes, the reaction endothermicity is reduced by more than 27 and 23 kcal/mol, respectively. Second, Figure 1 indicates that the transition state shifts toward the reactants and is stabilized giving a reduced activation energy in agreement with the Hammond postulate.<sup>46,47</sup> Within the (8,0) and (9,0) carbon nanotubes, the reaction barrier is decreased by an estimated 13 and 12 kcal/mol, respectively.

In predicting electronic response properties such as the polarizability, the quality of the basis set employed is the most important factor in obtaining quantitative results.<sup>48–50</sup> In the present work, the use of a basis set more extensive than 3-21G to represent the carbon nanotubes would have proved too costly. For calibration sake, polarizability calculations were carried out for  $C_{60}$ . The B3PW91/3-21G level of theory underestimates the electronic polarizability of  $C_{60}$  ( $64.9 \text{ \AA}^3$ ) by approximately 15%, compared to a recent experimental determination ( $76.5 \text{ \AA}^3$ ).<sup>51</sup> Therefore, the stabilizing effect on dipolar species inside carbon nanotubes may be underestimated in the current work by a proportional amount.

**Proximity Effect.** In addition to the effect on relative reaction enthalpies of being inside carbon nanotubes, it is of general interest to investigate the stabilizing effect on dipolar reactions of being in the proximity of graphitic materials. For example, reaction enthalpies for chemical species in the interstitial spaces between carbon nanotubes, on a graphite surface, or in a thin film of  $C_{60}$  molecules could be affected in a similar fashion as those inside carbon nanotubes. To provide an estimate of the proximity effect, calculations were carried out using a small graphite sheet.

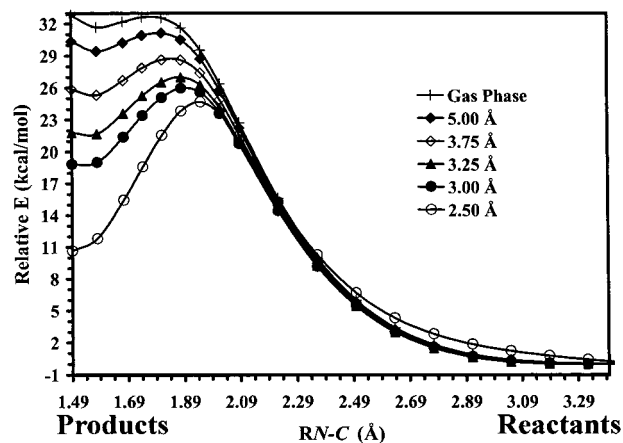


**Figure 3.** Gas-phase potential energy curve for the Menshutkin  $S_N2$  reaction and energy curves for the gas-phase structures at distances of 5.00, 3.75, 3.25, 3.00, and 2.50 Å from a  $C_{42}H_{18}$  graphene sheet.

A hydrogen-terminated fragment of a graphite sheet,  $C_{42}H_{18}$ , was fully optimized within  $D_{2h}$  symmetry at the B3PW91/3-21G level of theory. For each of the gas-phase optimized reaction path structures linking the Menshutkin reactant dipole complex and the ion pair product, single-point calculations were performed fixing the  $C_{3v}$  symmetry axis of the reaction system at various distances from the graphite sheet. The resulting potential energy curves for 5.00, 3.75, 3.25, 3.00, and 2.50 Å from the graphite sheet are shown in Figure 3, along with the gas-phase curve for comparison. The potential energy curves in the range 5.00–2.50 Å bridge the gap between the gas-phase relative energies and those closely resembling the nanotube-confined reaction path curves. The stabilizing effect of close proximity to a graphitic structure on dipolar species is clear. The reaction barrier and overall endothermicity are reduced by ca. 1.5 and 2.2, 4.0 and 6.4, 5.6 and 10.0, 6.6 and 12.8, and 7.9 and 21.0 kcal/mol for the distances 5.00, 3.75, 3.25, 3.00, and 2.50 Å, respectively.

#### Polarizable Continuum Models of Nanotube Confinement.

Theoretical investigations of the effect of solvation on chemical reactivity and molecular properties often use a polarizable continuum model (PCM) because of its simplicity, flexibility, and efficiency. In a PCM calculation,<sup>52</sup> the reacting system is placed inside a cavity embedded in a polarizable continuum with a fixed dielectric constant characteristic of the polar solvent. Given the physical nature of the composite molecule/carbon nanotube system considered here, it is reasonable to expect to recover a significant fraction of the stabilizing effect by using such an approach.

To employ a PCM approach to evaluate its capability to model the effects of nanotube confinement on the Menshutkin relative energies, effective dielectric constants must be derived for the (8,0) and (9,0) nanotubes used here. The optical dielectric constant of a medium is determined by its polarizability through the Clausius–Mossotti relation:<sup>53–55</sup>

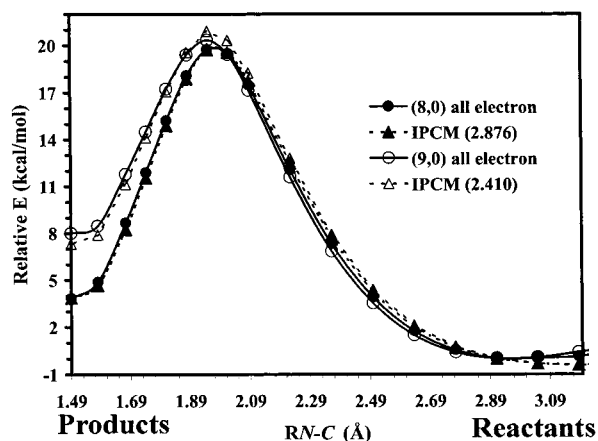
$$\epsilon = 1 + \rho\alpha(1 - \frac{1}{3}\rho\alpha)^{-1} + \frac{1}{3}\rho^2\alpha^2$$

where  $\rho$  is the number density of the constituents and  $\alpha$  is the polarizability.

The polarizability of the (8,0) and (9,0) carbon nanotubes, calculated at the B3PW91/3-21G level of theory, is summarized in Table 2. The axial polarizability for both nanotubes is calculated to be roughly three times larger than the radial polarizability, with an axial polarizability per carbon atom of ca.  $3.80$  and  $3.54 \text{ \AA}^3$  for the (8,0) and (9,0) nanotubes. From

**TABLE 2: Polarizabilities for the (8,0) and (9,0) Carbon Nanotubes Computed at the B3PW91/3-21G Level of Theory**

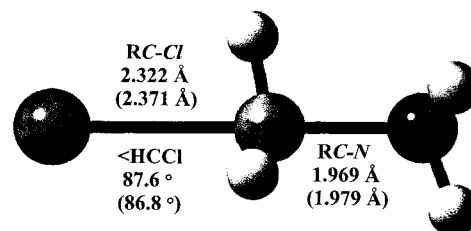
	(8,0) carbon nanotube	(9,0) carbon nanotube
stoichiometry	C <sub>96</sub> H <sub>16</sub>	C <sub>108</sub> H <sub>18</sub>
symmetry	D <sub>8h</sub>	D <sub>9h</sub>
tube diameter (Å)	6.35	7.12
polarizability		
$\alpha_{xx} = \alpha_{yy}$ (Å <sup>3</sup> )	136.22	138.06
$\alpha_{xy} = \alpha_{yz} = \alpha_{zx}$ (Å <sup>3</sup> )	0.00	0.00
$\alpha_{zz}$ (Å <sup>3</sup> )	365.04	382.12
$\alpha_{zz}$ per C atom (Å <sup>3</sup> )	3.80	3.54
isotropic $\alpha$ (Å <sup>3</sup> )	212.49	219.41
effective dielectric constant	2.876	2.410

**Figure 4.** Energy curves for the Menshutkin S<sub>N</sub>2 reaction gas-phase structures inside the (8,0) and (9,0) carbon nanotubes and in isodensity polarizable continuum models using the derived effective dielectric, for comparison.

the optimized geometries, the (8,0) and (9,0) carbon nanotubes have a C to C inner volume of 359.9 Å<sup>3</sup> and 453.1 Å<sup>3</sup>, respectively. Through the use of the Clausius–Mossotti relation, the effective dielectric constants for chemical processes inside the (8,0) and (9,0) carbon nanotubes are 2.876 and 2.410.

To evaluate the effectiveness of a PCM approach in modeling the effect of nanotube confinement on the Menshutkin S<sub>N</sub>2 enthalpies and activation energies, isodensity polarizable continuum model calculations were carried out for the gas-phase reaction path structures using the derived effective dielectric constants. For the isodensity polarizable continuum model (IPCM),<sup>42</sup> the cavity shape is determined by the electronic isodensity surface (0.0004 e/au<sup>3</sup>) of the H<sub>3</sub>N + H<sub>3</sub>CCl structures. The potential energy profiles using IPCM (2.876) and IPCM (2.410) are shown in Figure 4, along with the all electron (8,0) and (9,0) carbon nanotube confined results for comparison. The agreement between the all electron and the IPCM energies is impressive, confirming the stabilization mechanism. The effective dielectric IPCM energies for the Menshutkin relaxed path structures are within 1 kcal/mol of the all electron nanotube-confined energies.

The transition state for the Menshutkin S<sub>N</sub>2 reaction was optimized using an effective dielectric model ( $\epsilon = 2.410$ ) and inside the (9,0) carbon nanotube for comparison as an additional test of the performance of the effective dielectric approach for modeling the effect of carbon nanotube confinement. Inside the (9,0) carbon nanotube, the transition state was optimized neglecting the nanotube degrees of freedom, aligning the symmetry axes of the Menshutkin reaction system and carbon nanotube, and fixing the methyl carbon at the center of the nanotube. The effective dielectric transition state was optimized using the simplest reaction field model, the Onsager dipole

**Figure 5.** Menshutkin S<sub>N</sub>2 transition state geometric parameters optimized inside the (9,0) carbon nanotube and using the Onsager model using the derived effective dielectric of  $\epsilon = 2.410$  (in parentheses).

model,<sup>41</sup> which includes only dipole interactions and uses a spherical cavity shape. The Onsager transition state was verified by a subsequent frequency calculation, which gave a single imaginary frequency. Work by Foresman et al.<sup>42</sup> has shown that the simple Onsager dipole model satisfactorily recovers most of the geometry changes due to solvent effects. The transition state geometric parameters from the all electron calculation optimized inside the (9,0) carbon nanotube are shown in Figure 5, along with the Onsager results (in parentheses) for comparison. The structures from the two treatments are in good agreement, lending further support for the effectiveness of dielectric calculations to model the effect of carbon nanotube confinement.

The (9,0) carbon nanotube confined reaction barrier can be calculated by comparing the energy of the optimized Onsager transition state structure calculated using IPCM (2.410) to the IPCM energies for the structures early on the gas-phase reaction path. A comparison yields a reaction barrier of ca. 19.2 kcal/mol, which is reduced from the gas-phase barrier by ca. 13.5 kcal/mol. This value is comparable to the barrier derived from the all electron nanotube-confined gas-phase reaction path results and is in good agreement (within 0.5 kcal/mol) with the barrier calculated from the fully optimized transition state inside the (9,0) carbon nanotube, which gives a barrier of ca. 18.7 kcal/mol.

Optimization of the transition state using the Onsager model followed by an IPCM energy calculation using the effective dielectric constant derived for the (8,0) carbon nanotube gives a reaction barrier of 17.7 kcal/mol, which is reduced from the gas-phase barrier by ca. 15 kcal/mol. The Onsager optimized transition state structural parameters and IPCM barrier heights using the effective dielectric constants are summarized in Table 1.

## Conclusions

The effect of confinement inside (8,0) and (9,0) carbon nanotubes on the Menshutkin S<sub>N</sub>2 reaction enthalpies and activation energy was investigated using hybrid density functional theory. Inside the carbon nanotubes, the reaction barrier and overall endothermicity is significantly reduced compared to that in the gas phase. The proximity effect on dipolar stabilization by a small graphite sheet was also examined. Effective dielectric constants for use in polarizable continuum models of confinement inside the (8,0) and (9,0) nanotubes were derived from the nanotube polarizabilities. The polarizable continuum calculations provided results in excellent agreement with the all electron calculations, confirming the stabilization mechanism and offering a cost-effective approach to exploring further nanotube-confined chemistries. Overall, the effect of confinement of a reaction system inside a carbon nanotube closely resembles solvation in a low-dielectric solvent. Chemical reactions in which there is a large separation of charge along

the reaction coordinate may be enhanced inside fullerene-based materials because of their large polarizabilities.

**Acknowledgment.** H.B.S. and M.D.H. gratefully acknowledge financial support from the National Science Foundation (Grant No. CHE9874005) and a grant for computing resources from NCSA (Grant No. CHE980042N). M.D.H. would also like to thank the Department of Chemistry and the Graduate School, Wayne State University, for financial support provided by a Wilfried Heller Fellowship and a Summer 2001 Dissertation Fellowship.

**Supporting Information Available:** Tables of structural parameters. This material is available free of charge via the Internet at <http://pubs.acs.org>.

## References and Notes

- Iijima, S. *Nature* **1991**, *354*, 56.
- Odom, T. W.; Huang, J. L.; Kim, P.; Lieber, C. M. *J. Phys. Chem. B* **2000**, *104*, 2794.
- Hu, J. T.; Odom, T. W.; Lieber, C. M. *Acc. Chem. Res.* **1999**, *32*, 435.
- Saito, R.; Dresselhaus, G.; Dresselhaus, M. S. *Physical Properties of Carbon Nanotubes*; Imperial College Press: London, 1998.
- Rao, C. N. R.; Satishkumar, B. C.; Govindaraj, A.; Nath, M. *ChemPhysChem* **2001**, *2*, 78.
- Lu, J. P. *Phys. Rev. Lett.* **1997**, *79*, 1297.
- Treacy, M. M. J.; Ebbesen, T. W.; Gibson, J. M. *Nature* **1996**, *381*, 678.
- Yu, M.-F.; Lourie, O.; Dyer, M. J.; Moloni, K.; Kelly, T. F.; Ruoff, R. S. *Science* **2000**, *287*, 637.
- Yu, M.-F.; Files, B. S.; Arepalli, S.; Ruoff, R. S. *Phys. Rev. Lett.* **2000**, *84*, 5552.
- Hamada, N.; Sawada, S.; Oshiyama, A. *Phys. Rev. Lett.* **1992**, *68*, 1579.
- Mintmire, J. W.; Dunlap, B. I.; White, C. T. *Phys. Rev. Lett.* **1992**, *68*, 631.
- Saito, R.; Fujita, M.; Dresselhaus, G.; Dresselhaus, M. S. *Appl. Phys. Lett.* **1992**, *60*, 2204.
- Odom, T. W.; Huang, J.-L.; Kim, P.; Lieber, C. M. *Nature* **1998**, *391*, 62.
- Ugarte, D.; Chatelain, A.; deHeer, W. A. *Science* **1996**, *274*, 1897.
- Sloan, J.; Novotny, M. C.; Bailey, S. R.; Brown, G.; Xu, C.; Williams, V. C.; Friedrichs, S.; Flahaut, E.; Callender, R. L.; York, A. P. E.; Coleman, K. S.; Green, M. L. H. *Chem. Phys. Lett.* **2000**, *329*, 61.
- Chu, A.; Cook, J.; Heesom, R. J. R.; Hutchison, J. L.; Green, M. L. H.; Sloan, J. *Chem. Mater.* **1996**, *8*, 2751.
- Brown, G.; Bailey, S. R.; Sloan, J.; Xu, C.; Friedrichs, S.; Flahaut, E.; Coleman, K. S.; Hutchison, J. L.; Dunin-Borkowski, R. E.; Green, M. J. H. *Chem. Commun.* **2001**, 845.
- Smith, B. W.; Monthieux, M.; Luzzi, D. E. *Nature* **1998**, *396*, 323.
- Burteaux, B.; Claye, A.; Smith, B. W.; Monthieux, M.; Luzzi, D. E.; Fischer, J. E. *Chem. Phys. Lett.* **1999**, *310*, 21.
- Smith, B. W.; Monthieux, M.; Luzzi, D. E. *Chem. Phys. Lett.* **1999**, *315*, 31.
- Sloan, J.; Dunin-Borkowski, R. E.; Hutchison, J. L.; Coleman, K. S.; Williams, V. C.; Claridge, J. B.; York, A. P. E.; Xu, C. G.; Bailey, S. R.; Brown, G.; Friedrichs, S.; Green, M. L. H. *Chem. Phys. Lett.* **2000**, *316*, 191.
- Smith, B. W.; Luzzi, D. E. *Chem. Phys. Lett.* **2000**, *321*, 169.
- Kataura, H.; Maniwa, Y.; Kodama, T.; Kikuchi, K.; Hirahara, K.; Suenaga, K.; Iijima, S.; Suzuki, S.; Achiba, Y.; Kratschmer, W. *Synth. Met.* **2001**, *121*, 1195.
- Han, W.; Fan, S.; Li, Q.; Hu, Y. *Science* **1997**, *277*, 1287.
- Menshutkin, N. Z. *Phys. Chem.* **1890**, *5*, 589.
- Menshutkin, N. Z. *Phys. Chem.* **1890**, *6*, 41.
- Castejon, H.; Wiberg, K. B. *J. Am. Chem. Soc.* **1999**, *121*, 2139.
- Gao, J. *J. Am. Chem. Soc.* **1991**, *113*, 7796.
- Shaik, S.; Ioffe, A.; Reddy, A. C.; Pross, A. *J. Am. Chem. Soc.* **1994**, *116*, 262.
- Truong, T. N.; Truong, T. T. T.; Stefanovich, E. V. *J. Chem. Phys.* **1997**, *107*, 1881.
- Solà, M.; Lledós, A.; Duran, M.; Bertrán, J.; Abboud, J. L. M. *J. Am. Chem. Soc.* **1991**, *113*, 2873.
- Dillet, V.; Rinaldi, D.; Bertrán, J.; Rivail, J.-L. *J. Chem. Phys.* **1996**, *104*, 9437.
- Frisch, M. J.; Trucks, G. W.; Schlegel, H. B.; Scuseria, G. E.; Robb, M. A.; Cheeseman, J. R.; Zakrzewski, V. G.; Montgomery, J. A., Jr.; Stratmann, R. E.; Burant, J. C.; Dapprich, S.; Millam, J. M.; Daniels, A. D.; Kudin, K. N.; Strain, M. C.; Farkas, O.; Tomasi, J.; Barone, V.; Cossi, M.; Cammi, R.; Mennucci, B.; Pomelli, C.; Adamo, C.; Clifford, S.; Ochterski, J.; Petersson, G. A.; Ayala, P. Y.; Cui, Q.; Morokuma, K.; Malick, D. K.; Rabuck, A. D.; Raghavachari, K.; Foresman, J. B.; Cioslowski, J.; Ortiz, J. V.; Stefanov, B. B.; Liu, G.; Liashenko, A.; Piskorz, P.; Komaromi, I.; Gomperts, R.; Martin, R. L.; Fox, D. J.; Keith, T.; Al-Laham, M. A.; Peng, C. Y.; Nanayakkara, A.; Gonzalez, C.; Challacombe, M.; Gill, P. M. W.; Johnson, B. G.; Chen, W.; Wong, M. W.; Andres, J. L.; Head-Gordon, M.; Replogle, E. S.; Pople, J. A. *Gaussian 98*, revision A.6; Gaussian, Inc.: Pittsburgh, PA, 1998.
- Becke, A. D. *J. Chem. Phys.* **1993**, *98*, 5648.
- Perdew, J. P. In *Electronic Structure of Solids*; Ziesche, P., Eschrig, H., Eds.; Akademie Verlag: Berlin, 1991.
- Franci, M. M.; Petro, W. J.; Hehre, W. J.; Binkley, J. S.; Gordon, M. S.; Johnson, D. J.; Pople, J. A. *J. Chem. Phys.* **1982**, *77*, 3654.
- Hehre, W. J.; Ditchfield, R.; Pople, J. A. *J. Chem. Phys.* **1975**, *56*, 2257.
- Clark, T.; Chandrasekhar, J.; Spitznagel, G. W.; Schleyer, P. v. R. *J. Comput. Chem.* **1983**, *4*, 294.
- Binkley, J. S.; Pople, J. A.; Hehre, W. J. *J. Am. Chem. Soc.* **1980**, *102*, 939.
- Gordon, M. S.; Binkley, J. S.; Pople, J. A.; Pietro, W. J.; Hehre, W. J. *J. Am. Chem. Soc.* **1982**, *104*, 2797.
- Onsager, L. *J. Am. Chem. Soc.* **1938**, *58*, 1486.
- Foresman, J. B.; Keith, T. A.; Wiberg, K. B.; Snoonian, J.; Frisch, M. J. *J. Phys. Chem.* **1996**, *100*, 16098.
- Benedict, L. X.; Louie, S. G.; Cohen, M. L. *Phys. Rev. A* **1995**, *52*, 8541.
- Jensen, L.; Schmidt, O. H.; Mikkelsen, K. V.; Åstrand, P. O. *J. Phys. Chem. B* **2000**, *104*, 10462.
- Wan, X.; Dong, J.; Xing, D. Y. *Phys. Rev. B* **1998**, *58*, 6756.
- Hammond, G. S. *J. Am. Chem. Soc.* **1955**, *77*, 334.
- Issacs, N. S. *Physical Organic Chemistry*; Wiley: New York, 1987.
- Sadlej, A. J. *Collect. Czech. Chem. Commun.* **1988**, *53*, 1995.
- Perez, J. J.; Sadlej, A. J. *THEOCHEM* **1996**, *371*, 31.
- Dykstra, C. E. *Ab Initio Calculation of the Structure and Properties of Molecules*; Elsevier: Amsterdam, Netherlands, 1988.
- Antoine, R.; Dugourd, P.; Rayane, D.; Benichou, E.; Broyer, F.; Chandezon, M.; Guet, C. *J. Chem. Phys.* **1999**, *110*, 9771.
- Tomasi, J. In *Encyclopedia of Computational Chemistry*; Schleyer, P. v. R., Ed.; John Wiley & Son Ltd: New York, 1998; p 2547.
- Born, M.; Wolfe, E. *Principles of Optics*; Pergamon: Oxford, 1980; p 98.
- Kuz'min, V. I.; Romanov, V. P.; Zubkov, L. A. *Phys. Rep.* **1994**, *248*, 71.
- Morice, O.; Castin, Y.; Dalibard, J. *Phys. Rev. A* **1995**, *51*, 3896.